

Radiation Defects Created in *n*-Type 4H-SiC by Electron Irradiation in the Energy Range of 1–10 MeV

Pavel Hazdra* and Jan Vobecký

Radiation damage produced in 4H-SiC *n*-epilayers by electrons of different energies is presented. Junction barrier Schottky power SiC diodes are irradiated with 1.05, 2.1, 5, and 10 MeV electrons with doses up to 600 kGy. Radiation defects are characterized by capacitance deep-level transient spectroscopy and capacitance-to-voltage (*C*–*V*) measurement. Results, which are compared with previous data obtained on 4.5 MeV electrons, show that the damage structure is very similar for all irradiation energies. Dominating is the generation of simple, thermally unstable defects evidenced by the presence of acceptor levels located at 0.25, 0.38, 0.60, and 0.72 eV below the 4H-SiC conduction band edge. With increasing energy of electrons, the number of simple defects saturates, and the production of more complex, cluster-related defects grow. Majority of introduced defects are acceptor centers, which compensate *n*-type (nitrogen) doping of the epilayer. The carrier removal rate increases with electron energy and follows well the classical nonionization energy loss (NIEL) scaling for electrons in silicon. The stability of introduced defects and their effect on carrier lifetime reduction are discussed, as well.

1. Introduction

Recent progress in carrier lifetime enhancement in 4H-SiC epitaxial layers given by the disclosure of the Z1/Z2 defect origin and means of its suppression finally opens the way to the production of reliable bipolar SiC devices.^[1] The electron irradiation is a widely used technique to control the carrier lifetime in silicon power devices. On the one hand, it allows to improve electrical parameters, namely, to reduce the turn-off time, reverse recovery charge, or recovery loss. Consequently, the electron irradiation is widely used to adjust the ratio between the static and dynamic losses according to the application needs given by an end user. Using the same front-end process (the same final chip or wafer), the electron irradiation can be varied to carry out a faster device

with a higher ON-state voltage suitable for hard switching at two- or three-level power converters and a slower device with a lower ON-state voltage suitable for the modular multilevel converters switching at frequencies close to the fundamental output frequency of 50 Hz. On the other hand, the electron irradiation can be used to precisely match the relevant electrical parameters of devices operating in series or in parallel. For the serial operation, the electron irradiation is used to adjust the reverse recovery charge Q_{rr} of thyristors into a very narrow-band. The lower the Q_{rr} band is, the lower difference in maximal voltages during switching $\Delta V = \Delta Q_{rr}/C$ is achieved, where C is the capacitance of a parallel-connected snubber capacitor. This allows one to minimize the amount of redundant thyristors in high-voltage stacks to prevent a device breakdown. For a reliable parallel operation of devices, the electron irradiation can be used to bring the ON-state voltage drop


V_F into a narrow V_F -band, typically not larger than 50–100 mV for the average rating current measured at maximal junction temperature.

For the best utilization of the techniques summarized earlier, a detailed knowledge of defect structure, defect introduction rate, annealing behavior, and impact of individual defects on electrical parameters in the widest range of irradiation energy is needed. There are several reasons for that. As the wafers can have a thickness from 50 to 1500 μm , the energies with low and very high penetration depths are needed—the lower the energy, the lower the cost. The defect structure for very low and very high energies can be very different as well as its impact on relevant electrical parameters. For example, the highest available irradiation energy of electrons in the industry gives the best technology curve between the ON-state voltage and recovery charge of thyristors compared with the lower energies. In the high-voltage direct current systems with several thousand thyristors within a single valve, the impact on energy savings is significant. Also, in the case of fast recovery diode, a higher irradiation energy of electrons leads to a better technology curve between the ON-state voltage drop V_F and the reverse recovery energy loss E_{rec} . To achieve a similar point at the technology curve using the 1.05 MeV electrons, one needs about 2.7 times higher irradiation dose against 2.1 MeV electrons and about 5 times against 5 and 10 MeV electrons.

It is obvious that the aforementioned wide utilization of the lifetime control by the electron irradiation on silicon power

Prof. P. Hazdra, Prof. J. Vobecký
Department of Microelectronics
Faculty of Electrical Engineering
Czech Technical University in Prague
Technická 2, CZ-166 27 Prague 6, Czech Republic
E-mail: hazdra@fel.cvut.cz

Prof. J. Vobecký
ABB Switzerland Ltd. Semiconductors
Fabrikstrasse 3, Lenzburg CH-5600, Switzerland

 The ORCID identification number(s) for the author(s) of this article can be found under <https://doi.org/10.1002/pssa.201900312>.

DOI: 10.1002/pssa.201900312

devices can be analogically implemented on the future bipolar SiC power devices. For silicon material, the effect of electron irradiation on the radiation defect production and the resulting performance of electron devices is well researched.^[2,3] However, for the SiC, the aforementioned information is sparse. The aim of this contribution is to present the effect of electron irradiation on the low-doped *n*-type 4H-SiC epilayers in a wide range of projectile's energies. Although received on the combined bipolar-Schottky diode, the knowledge provided by this paper is also relevant for the body diodes of the low-voltage SiC MOSFETs (650, 1200, 1700 V, etc.) widely used in the current and future power converters. This is because they usually suffer from a poor reverse recovery performance of the intrinsic diodes, such as large recovery charge and high recovery peak current. As this could limit their usage in high-frequency applications, lifetime control can be helpful. Data obtained are also of key importance for nonionization energy loss (NIEL)^[4] characterization in 4H-SiC material.

2. Experimental Section

The effect of electron irradiation was investigated on 4H-SiC *n*-type epilayers ($N_D \approx 3.4 \times 10^{15} \text{ cm}^{-3}$) grown on heavily nitrogen-doped n^+ (0.025–0.028 $\Omega \text{ cm}$) 360 μm thick substrate. The epilayers formed 20 μm thick drift region of 10 A/1700 V junction barrier Schottky (JBS) power diode chips CPW3-1700-S010B produced by Cree, Inc.^[5] These matured devices with a low spread of relevant parameters allowed us to achieve consistent results while having a broad set of devices under test. Devices were irradiated with 1.05, 2.1, 5, and 10 MeV electrons in the dose range from 75 to 600 kGy (electron fluences from 3.1×10^{14} to $2.5 \times 10^{15} \text{ cm}^{-2}$) and with epilayer facing the electron beam. The irradiation was performed at Leoni Studer AG, Daeniken, Switzerland. The selected range of irradiation energies ends up at 10 MeV, which is the highest allowed industrial energy for safety reasons. The reference irradiation was performed by 4.5 MeV electrons using the electron linear accelerator LINAC 4-1200 with doses up to 2000 kGy.^[6] The capacitance-to-voltage (*C*-*V*) characteristics were measured prior to and after electron irradiation using the HP 4280A 1 MHz *C* Meter/*C*-*V* Plotter. The radiation defects and their thermal stability were characterized by capacitance deep-level transient spectroscopy (DLTS) using the spectrometers DLS-82E and DLS-83D from SEMILAB Inc. Our experimental equipment allowed us investigation of radiation defects up to the epilayer depth of 4 μm (DLTS) or 6 μm (*C*-*V*).

3. Results and Discussion

The effect of electron energy on the radiation defect introduction into the 4H-SiC *n*-type nitrogen-doped epitaxial layer is shown in Figure 1 where the majority carrier DLTS spectra of as irradiated samples (the electron dose of 300 kGy) are compared with the spectrum recorded prior to irradiation. As the majority of radiation defects introduced into the 4H-SiC by electron irradiation at room temperature is unstable and starts to anneal out already at temperatures higher than 50 °C,^[7,8] we present the DLTS spectra, which were recorded during the first temperature scan. This

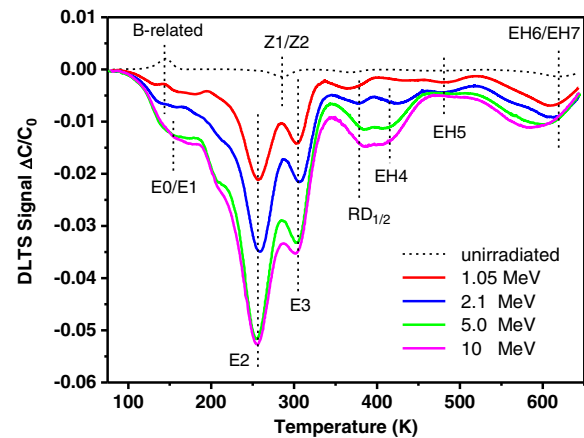


Figure 1. Majority carrier DLTS spectra measured in the *n*-type 4H-SiC epitaxial layer after electron irradiation with energies 1.05, 2.1, 5, and 10 MeV to a dose of 300 kGy, rate window 4.1 s⁻¹.

gives us the possibility to show all the defects, which were generated in 4H-SiC by the electron irradiation. Table 1 gives an overview about identification parameters (the energy position $E_C - E_T$ related to the conduction band edge and the electron capture cross section σ_n) of all detected levels and their possible identity.

In the spectrum of the unirradiated sample, we find three peaks related to deep levels, which are typical for high-quality *n*-type 4H-SiC epilayers:^[9] the boron acceptor level ($E_v + 0.25 \text{ eV}$) at $T = 145 \text{ K}$, the Z1/Z2 lifetime-limiting defect ($T = 285 \text{ K}$), and the deeply lying level EH6/EH7 ($T = 621 \text{ K}$). There was a long lasting discussion concerning origin of these two levels (see the study by Klein et al.^[10]); however, recent investigations^[11] showed that the Z1/Z2 and EH6/EH7 levels are related to different charge states of the carbon vacancy. The shallower state at $E_C - 0.68 \text{ eV}$, the Z1/Z2 center, is a double acceptor level ($=|0\rangle$). The first transition Z2 ($=|-$) is very fast so only the second transition Z1 ($=|-$) can be registered by the DLTS. Laplace DLTS investigation^[12] showed that the Z1 and Z2 transitions are related to the carbon vacancy at the hexagonal and pseudocubic sites of the lattice,

Table 1. Deep levels detected in 4H-SiC after electron irradiation and subsequent annealing.

Level	$E_C - E_T$ [eV]	σ_n [cm ²]	Reference
E0	0.25	2×10^{-17}	[7]
E1	0.38	6×10^{-13}	[7,15,16]
S1	0.43	4×10^{-14}	[8]
E2	0.60	4×10^{-14}	[7,15,16]
Z1/Z2	0.68	6×10^{-14}	[8,10,11,15]
E3	0.72	7×10^{-14}	[7,15,16]
S2	0.75	1×10^{-14}	[7,8]
RD _{1/2}	0.88	3×10^{-14}	[17,18]
EH4	1.03	2×10^{-13}	[8,10,16]
EH5	1.08	2×10^{-15}	[8,10,16]
EH6/EH7	1.58	6×10^{-13}	[8,10,11,13,16]

respectively. The deeper level EH6/EH7 at $E_C - 1.58$ eV was also analyzed by the Laplace DLTS,^[13] allowing separation of the overlapping emissions from levels EH6 and EH7. Results show that the EH6 and EH7 levels are, in fact, located 1.30 and 1.49 eV below the conduction band minimum, respectively. While level EH6 is related to a higher-order cluster involving the carbon vacancy, the EH7 transition is related to its donor transition $(0|+)$. This is because only the EH7 level is registered in 4H-SiC after irradiation with low-energy (210 keV) electrons.^[8,10] Both the Z1/Z2 and EH6/EH7 centers are stable defects, which anneal out at temperatures higher than 1300 °C.^[10]

The DLTS spectra measured after irradiation show that the electron irradiation in the energy range 1.05–10 MeV introduces a complex feature exhibiting local maxima at 150, 255, and 302 K. This feature is probably given by an overlap of several peaks (defects) with close activation energy. Unfortunately, low temperature stability of these defects does not allow detailed understanding of their origin. The maxima labeled E0/E1, E2, and E3 usually appear in different proportions in the DLTS spectra measured on the 4H-SiC irradiated by different particles (electrons, neutrons, protons, and alphas).^[8,10,17] They are related to point defects. For example, in the work,^[7] they are referenced as levels S1/S2, S3, and S4. The dominant feature usually splits into two peaks E2($E_C - 0.60$ eV) and E3($E_C - 0.72$ eV) accompanied by a satellite E0/E1 composed by contribution of two levels E0($E_C - 0.25$ eV) and E1($E_C - 0.38$ eV) with substantially different electron capture cross sections. While level E1 is attributed to the carbon interstitial (C_i), the origin of the E0 peak is still under discussion.

DLTS peaks appearing on the right-hand side of spectra are related to silicon vacancies and more complicated defects (clusters). The peak at $T = 380$ K labeled $RD_{1/2}$ was attributed to the positively charged silicon vacancy V_{Si}^+ ^[14] and represents one of the dominant defect centers in the neutron irradiated 4H-SiC. The level giving the maximum at $T = 415$ K is identical to level EH4 reported in the previous studies.^[8,10] This level is related to a higher-order defect cluster because it has been detected after the 2.5 MeV electron irradiation at fluences higher than 10^{14} cm⁻² but it was absent in the 4H-SiC irradiated with low-energy (80–250 keV) electrons. The level peaking at $T = 480$ K has the same characteristics as the center EH5 detected in the electron or proton irradiated 4H-SiC annealed at 300 °C.^[8,10] Both the EH4 and EH5 defects are stable at operation temperatures of power devices (below 200 °C) and anneal out between 400 and 600 °C.^[10] The broad feature peaking at $T = 600$ K is then given by the contribution of the aforementioned levels EH6/EH7.^[8,10]

DLTS spectra, i.e., the damage structure presented in Figure 1, are very similar. The number of defects grows as electron energy increases. However, the number of point defects (evidenced by peaks E0/E1, E2, and E3) starts to saturate at the electron energy of 10 MeV, whereas the signal of level $RD_{1/2}$, EH4, and probably also of the EH6 level continues to grow. This is proof that, likewise in the case of silicon,^[3] the ratio between the concentrations of cluster-related defects and point defects increases with electron energy.

As mentioned earlier, the majority of radiation defects introduced into 4H-SiC by electron irradiation at room temperature is unstable and disappears or transforms to another defects by

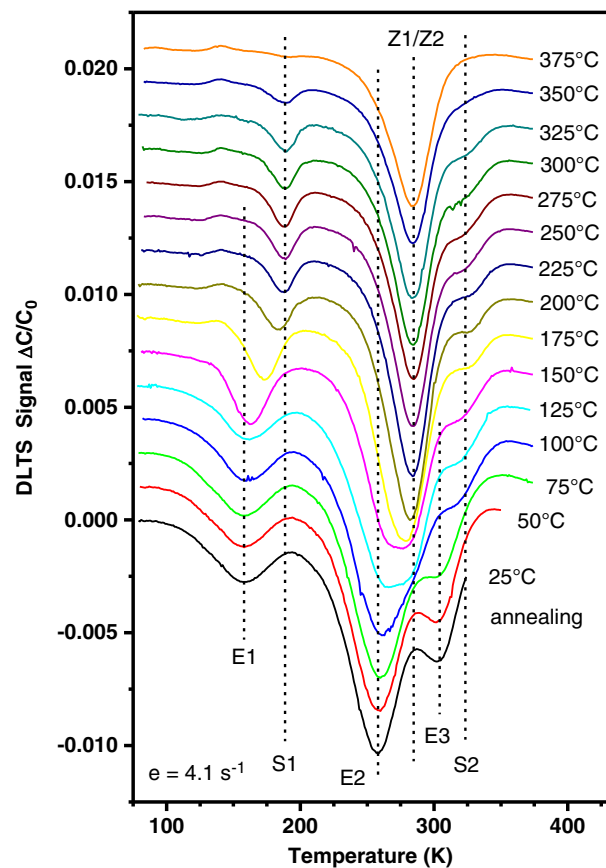


Figure 2. Majority DLTS spectra measured in the *n*-type 4H-SiC epitaxial layer with 200 kGy of 4.5 MeV electrons after different stages of 30 min isochronal annealing at temperatures ranging from 25 to 375 °C, rate window 4.1 s⁻¹.

annealing between 50 and 400 °C. This is shown in Figure 2, which presents, in detail, the effect of low-temperature isochronal annealing on DLTS spectra recorded on 4H-SiC epilayers irradiated with 4.5 MeV electrons. Increasing the temperature above 50 °C causes first the fast disappearance (the shift in temperature position) of the E2 level, which gradually transforms to the Z1/Z2 center. At about 125 °C, the E1 and E3 peaks start to transform. First, they narrow, and, at about 175 °C, they shift to higher temperatures (to the right). Deep levels connected with the new peaks (S1 and S2) have been found to exhibit a one-to-one relation and are proposed to be two charge states of the same acceptor center, labeled as the S-center.^[19] The S-center then anneals out above 350 °C by the first-order annealing process with an activation energy of 1.8 eV.^[19] The E1 → S1, E2 → Z1/Z2, and E3 → S2 transformation occurring in the 50–225 °C temperature range has been reported by several studies^[7,8,10,16,18,20,21] but no conclusive explanation exists. At first, it was considered that the aforesaid DLTS spectra transformation might be the result of dissociation or migration and complexing of radiation defects.^[20] Detailed investigation^[21] has shown that the change in spectra is caused by a change in the emission rate given by the energy difference between the trap level and conduction band edge. As all levels are shifted, the change is more likely

related to the surrounding material rather than to defect themselves. One reason for the conduction band edge shift may be the generation of 3C polytype, which has a smaller bandgap due to the formation of stacking faults directly after irradiation. The 3C regions are annealed by heat treatment between 100 and 200 °C, and this can increase the energy difference between the trap level and conduction band edge. Another possible explanation can be the strain caused by a large number of point defects (interstitials) generated by irradiation, which can affect the defect levels observed by DLTS.^[21]

The maximal rating temperature of SiC power devices is expected to exceed 200 °C and correspondingly more under the overload conditions such as short circuit operation and during bonding of SiC chips into the substrates of power modules. Consequently, the annealing temperatures higher than 370 °C are necessary to stabilize the radiation damage produced by the electron irradiation. The carrier lifetime tailoring using this technique is a back-end process, which is applied after complete fabrication of the power device chip. This means that the post irradiation annealing should not damage any of the previously created layers, such as contacts, passivation and protection layers, etc. In our case, we used 370 °C annealing for 30 min to stabilize the defects introduced by the electron irradiation. This temperature provides the highest possible stability without damaging the CPW3-1700-S010B diode chips. The effect of the 370 °C annealing on the DLTS spectra of the diodes irradiated with the minimal (1.05 MeV) and maximal (10 MeV) electron energy is shown in **Figure 3**. Results show that the Z1/Z2 lifetime-limiting and very stable defect dominates the spectra of annealed samples. The Z1/Z2 center is accompanied by the deeply lying level EH6/7, which is the most efficient carrier generation center, and level EH5. The increased electron energy then makes the spectrum of annealed samples more complex: the number of deep levels increases due to the introduction of more stable defect clusters (EH4, EH5, and EH6 as the shoulder of the EH6/EH7 peak). Anyway, the most dominant stay the Z1/Z2 and EH6/EH7 defects thermally stable above 1300 °C with introduction rate proportional to the electron energy. The excellent thermal stability and the scaling of defect concentration with energy and dose thus determine the application potential of electron irradiation for the carrier lifetime control in SiC.

The defect profiles measured by DLTS showed that, in the range of electron energies under investigation, deep levels introduced by irradiation are homogeneously distributed in the epilayer. The fluence dependence of E1–E3 and Z1/Z2 defects is linearly dependent on the irradiation fluence up to the dose of 150 kGy, and the introduction rates can then be calculated as the ratio $dN_T/d\Phi$ between the defect concentration N_T and irradiation fluence Φ . **Table 2** presents the impact of the electron irradiation energy on the introduction rate of the dominant-level E2 measured on as-irradiated samples. The transformation $E2 \rightarrow Z1/Z2$ shown in Figure 2 is also considered by adding the resulting introduction rate of Z1/Z2 centers measured after 370 °C annealing. The results show that the introduction rates of both dominant lifetime killing defects (E2 and Z1/Z2) increase with irradiation energy and start to saturate at 10 MeV. Compared with silicon, the defect introduction rates in 4H-SiC are higher. For example, the irradiation with 10 MeV electrons introduces the E2 centers in 4H-SiC with a rate of

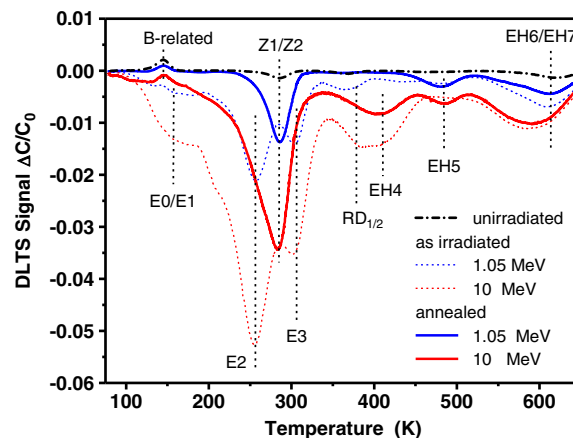


Figure 3. Majority carrier DLTS spectra measured in the *n*-type 4H-SiC epitaxial layer after electron irradiation with energies 1.05 and 10 MeV to the dose of 300 kGy (dashed) and subsequent 30 min annealing at 370 °C (solid), rate window 4.1 s^{−1}.

Table 2. The carrier removal rate K_N , the introduction rates of the E2 level $dn_{E2}/d\Phi$ (as irradiated samples), and the introduction rates of the Z1/Z2 level $dn_{Z1/Z2}/d\Phi$ (370 °C annealing for 30 min) versus the electron energy.

Energy [MeV]	As irradiated K_N [cm ^{−1}]	As irradiated $dn_{E2}/d\Phi$ [cm ^{−1}]	Annealed (370 °C) $dn_{Z1/Z2}/d\Phi$ [cm ^{−1}]
1.0	0.148	0.177	0.117
2.1	0.341	0.290	0.139
5.0	0.531	0.415	0.168
10	0.655	0.439	0.177

0.439 cm^{−1}, whereas the same irradiation of silicon introduces the dominant recombination centers with a rate of 0.14 cm^{−1} (vacancy-oxygen centers) and 0.05 cm^{−1} (divacancies).^[2]

The displacement damage produced by electron irradiation causes three dominant phenomena that usually lead to the degradation of irradiated power devices: the carrier removal in the *n*-type drift region and the decrease in carrier mobility and carrier lifetime.

The first effect, the carrier removal in *n*-type layers, is typical both for silicon and silicon carbide. In our case, the temperature-dependent $C-V(T)$ measurement (see **Figure 4**) revealed that the majority of deep levels introduced in the 4H-SiC by electron irradiation (Z1/Z2 and E0–E3 centers) exhibits an acceptor character. **Table 3** summarizes the introduction rates of these centers for irradiation with 4.5 MeV electrons. The $C-V(T)$ measurements are dominated by level E0, which is not obvious in the DLTS spectra shown in Figure 1. This acceptor level is located 0.25 eV below the conduction band and, compared with levels E1–E3, has a very small capture cross section. The capture of electrons on this level is very slow, and the E0 peak is then fully covered by the DLTS signal of level E1. Levels E1–E3 are deep enough to be negatively charged in the temperature range of power device operation (−50–150 °C), but the E0 center changes its charge state from negative to neutral at these temperatures. This causes a strong temperature dependence of electron

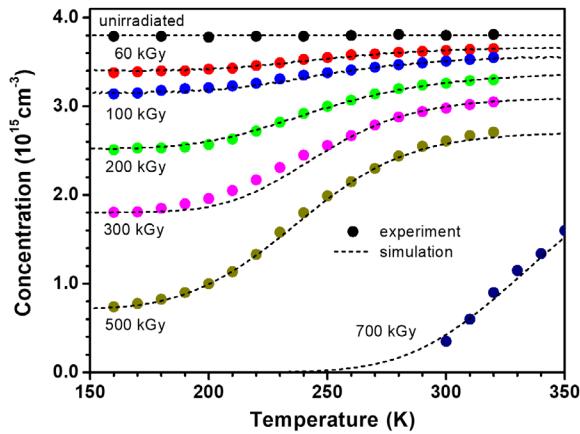


Figure 4. Temperature dependence of the free carrier (electron) concentration in the 4H-SiC epilayer forming the drift region of the JBS diodes (C3D10170H) irradiated with different doses of 4.5 MeV electrons.

Table 3. Introduction rates of dominant deep levels in the 4H-SiC irradiated by 4.5 MeV electrons (doses up to 200 kGy).

Level	$E_C - E_T$ [eV]	$dn_T/d\Phi$ [cm ⁻²]
E0	0.25	0.92
E1	0.38	0.13
E2	0.60	0.32
E3	0.74	0.10

concentration in the *n*-type epitaxial layer, especially at high irradiation doses. This is shown in Figure 4 where the measured values of carrier concentrations are compared with the results of simulation accounting for levels E0–E3 and their parameters presented in Table 3.

Due to the introduction of acceptor levels, an increase in the electron dose causes a gradual decrease in electron concentration *n* in the *n*-epilayer according to the formula

$$n = n_0 - K_N \Phi \quad (1)$$

where K_N is the carrier removal rate and Φ is the particle fluence. This linear decrease in carrier concentration with an increasing dose of electrons is shown in Figure 5 for different electron energies. The linear relationship is valid for low doses (fluence). At higher fluences, deviations may occur due to the change in the dominant type of the acceptor center.^[6] The measured carrier removal rates in the *n*-type 4H-SiC epitaxial layer for different energies of electrons are listed in Table 2 and shown in Figure 6 where they are compared with the literature data and the calculated nonionizing energy loss (NIEL) for electrons in silicon.^[21] Results show that the energy dependence of K_N scales well with the “classical” NIEL.

The second effect of electron irradiation, the mobility degradation, is more pronounced in the SiC than in silicon, where it takes place only at very high irradiation doses. Our previous investigations showed that the electron mobility in the 4H-SiC epilayer significantly decreases with irradiation dose as a result

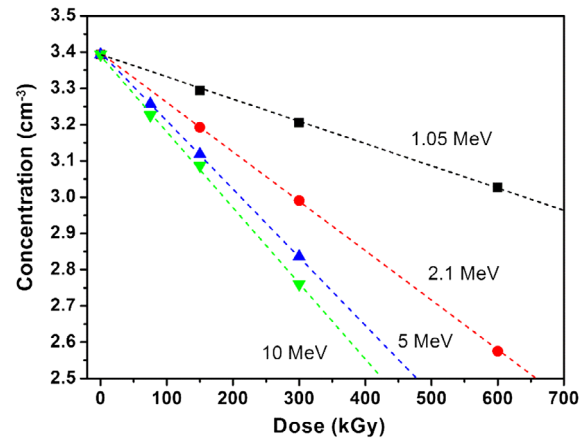


Figure 5. Decrease in electron concentration in the *n*-type 4H-SiC epitaxial layer with increasing dose of electron irradiation with electron energies 1.05, 2.1, 5, and 10 MeV (room temperature measurement).

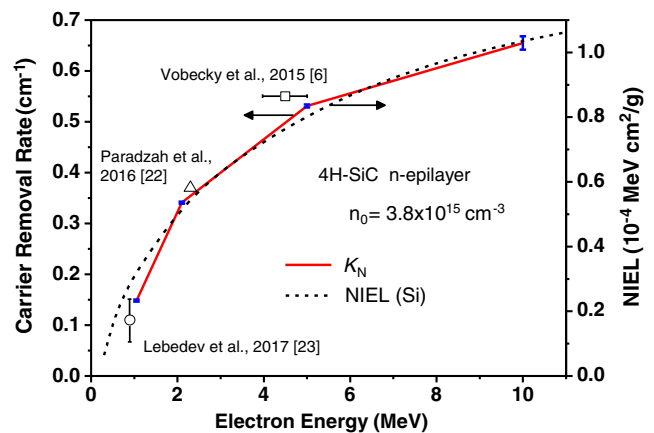


Figure 6. Carrier removal rates in the *n*-type 4H-SiC epitaxial layer versus the energy of electron irradiation: measured (line) and literature (points) data.^[6,22,23] The corresponding NIEL values for silicon (dashed line)^[24] are shown for reference.

of increased concentration of radiation defects.^[6] For the 4.5 MeV electrons, a significant mobility degradation can be observed at doses higher than 300 kGy. Unfortunately, the radiation doses used in this experiment are relatively low to show this effect relevantly.

The third effect, the degradation of carrier lifetime τ by deep levels introduced by the electron irradiation, is critical to the operation of bipolar devices. The decrease in carrier lifetime means shorter diffusion lengths and subsequent loss of the conductivity modulation in the low-doped *N*-type region, which leads to a sharp increase in the forward voltage drop during the ON-state regime of device operation. The decrease is proportional to the number of introduced defects and their carrier capture cross sections expressed by the lifetime degradation coefficient K_T ^[25]

$$\frac{1}{\tau} = \frac{1}{\tau_0} + K_T \Phi \quad (2)$$

where τ_0 is the original value of lifetime of an unirradiated device and Φ is the particle fluence. Due to the higher defect introduction rates in SiC, the values of the lifetime degradation coefficient are higher compared with silicon, e.g., $K_T = 3 \times 10^{-7} \text{ s}^{-1} \text{ cm}^2$ for the irradiation of 4H-SiC with 4.5 MeV electrons.^[6] On the other hand, the effect of increased recombination in SiC is first covered by generally lower values of τ_0 (1–10 μs) in the SiC epilayers. If we want to use the electron irradiation for lifetime control in SiC power devices, we have to consider the effect of annealing, which is always necessary for the long term thermal stabilization of defects (lifetime). As mentioned earlier, the annealing used in our experiment (370 °C) provides a single recombination center, the Z1/Z2 defect. Its capture cross section (see Table 1) and introduction rates (see Table 2) then give for the electron energies 1.05 and 10 MeV the lifetime degradation coefficients $K_T = 0.6 \times 10^{-7} \text{ s}^{-1} \text{ cm}^2$ and $K_T = 1 \times 10^{-7} \text{ s}^{-1} \text{ cm}^2$, respectively. For these degradation coefficients, the electron dose of a few kGy is sufficient to control the carrier lifetime over the entire range required by the SiC power devices.^[26]

Finally, we should mention that the degradation of the generation lifetime in 4H-SiC, which is related to the introduction of the generation centers (namely, the EH6/EH7 level lying close to the middle of the 4H-SiC bandgap), is not so important for device operation. The wide bandgap of 4H-SiC guarantees extremely low values of carrier generation rates, and the leakage current of irradiated devices usually stays within device specification. It is rather the increasing forward voltage drop (decreasing carrier mobility) with increasing temperature, which is going to limit the maximal rating temperature of SiC power devices in the future. It is also worth mentioning that the electron irradiation with doses up to 700 kGy has a negligible effect on the metal–semiconductor barrier height and the ideality factor of the JBS diode as shown in our previous studies.^[6]

4. Conclusions

The radiation defects from electron irradiation in the 4H-SiC JBS diode were characterized, considering the full range of irradiation energy available in the industry and the practical need to know their thermal stability up to 375 °C. Nine deep levels were identified in as-irradiated devices. Four (10 MeV electron irradiation) resp. three (1.05 MeV electron irradiation) deep levels remained after annealing at 375 °C. Among them are the most dominant Z1/Z2 and EH6/EH7 defects with introduction rate proportional to the electron energy, which are known to be thermally stable above 1300 °C. The excellent thermal stability and the scaling of defect concentration with the energy and dose determine the application potential of electron irradiation for the carrier lifetime control in the SiC. While the defect introduction rate is shown higher in the SiC compared with silicon, the saturation of this rate toward the energy of 10 MeV is similar in both SiC and silicon. The temperature-dependent C–V measurement revealed that the majority of deep levels introduced in the 4H-SiC by electron irradiation (Z1/Z2 and E0–E3 centers) exhibits an acceptor character, leading to carrier removal rate proportional to the dose and energy of electron irradiation. A comparison with published data and the calculated nonionizing

energy loss (NIEL) for electrons in silicon shows that the energy dependence of K_N in the SiC scales well with the “classical” NIEL.

Acknowledgements

This work was supported by the grant P102/12/2108 of the Czech Science Foundation (GACR) and the EU FP7 NMP 604057 project SPEED.

Conflict of Interest

The authors declare no conflict of interest.

Keywords

electron irradiation, lifetime control, radiation defects, silicon carbide

Received: April 15, 2019

Revised: June 6, 2019

Published online: July 24, 2019

- [1] M. Bakowski, P. Ranstad, J. K. Lim, W. Kaplan, S. A. Reshanov, A. Schoner, F. Giezendanner, A. Ranstad, *IEEE Trans. Electron Devices* **2015**, 62, 366.
- [2] R. Radu, I. Pintilie, L. C. Nistor, E. Fretwurst, G. Lindstroem, L. F. Makarenko, *J. Appl. Phys.* **2015**, 117, 164503.
- [3] R. Radu, E. Fretwurst, R. Klanner, G. Lindstroem, I. Pintilie, *Nucl. Instrum. Methods Phys. Res. A* **2013**, 730, 84.
- [4] P. Arnolda, C. Inguibert, T. Nuns, C. B. Pollo, *IEEE Trans. Nucl. Sci.* **2011**, 58, 756.
- [5] Cree, Inc., CPW3-1700S010 – Silicon Carbide Schottky Diode Chip, <https://www.wolfspeed.com/power/products/sic-schottky-diodes/cpw3-1700-s010b> (accessed: April 2019).
- [6] J. Vobecký, P. Hazdra, S. Popelka, R. K. Sharma, *IEEE Trans. Electron Devices* **2015**, 62, 1964.
- [7] A. Castaldini, A. Cavallini, L. Rigutti, F. Nava, *Appl. Phys. Lett.* **2004**, 85, 3780.
- [8] G. Alfieri, E. V. Monakhov, B. G. Svensson, A. Hallén, *J. Appl. Phys.* **2005**, 98, 113524.
- [9] P. B. Klein, B. V. Shanabrook, S. W. Huh, A. Y. Polyakov, M. Skowronski, J. J. Sumakeris, M. J. O’Loughlin, *Appl. Phys. Lett.* **2006**, 88, 052110.
- [10] G. Alfieri, E. V. Monakhov, B. G. Svensson, M. K. Linnarson, *J. Appl. Phys.* **2005**, 98, 043518.
- [11] N. T. Son, X. T. Trinh, L. S. Løvlie, B. G. Svensson, K. Kawahara, J. Suda, T. Kimoto, T. Umeda, J. Isoya, T. Makino, T. Ohshima, E. Janzén, *Phys. Rev. Lett.* **2012**, 109, 187603.
- [12] I. Capan, T. Brodar, J. Coutinho, T. Ohshima, V. P. Markevich, A. R. Peaker, *J. Appl. Phys.* **2018**, 124, 245701.
- [13] G. Alfieri, T. Kimoto, *Appl. Phys. Lett.* **2013**, 102, 152108.
- [14] F. Nava, A. Castaldini, A. Cavallini, P. Errani, V. Cindro, *IEEE Trans. Nucl. Sci.* **2006**, 53, 2977.
- [15] L. Storasta, J. P. Bergman, E. Janzén, A. Henry, J. Lu, *J. Appl. Phys.* **2004**, 96, 4909.
- [16] C. Hemmingsson, N. T. Son, O. Kordina, J. P. Bergman, E. Janzén, J. L. Lindström, S. Savage, N. Nordell, *J. Appl. Phys.* **1997**, 81, 6155.
- [17] T. Dalibor, G. Pensl, H. Matsunami, T. Kimoto, W. J. Choyke, A. Schöner, N. Nordell, *Phys. Stat. Sol. A* **1997**, 162, 199.
- [18] G. Izzo, G. Litrico, L. Calcagno, G. Foti, F. La Via, *J. Appl. Phys.* **2008**, 104, 093711.

- [19] M. L. David, G. Alfieri, E. V. Monakhov, A. Hallén, C. Blanchard, B. G. Svensson, J. F. Barbot, *J. Appl. Phys.* **2004**, 95, 4278.
- [20] J. P. Doyle, M. K. Linnarsson, P. Pellegrino, N. Keskitalo, B. G. Svensson, A. Schöner, N. Nordell, J. L. Lindström, *J. Appl. Phys.* **1998**, 84, 1354.
- [21] H. Kortegaard Nielsen, *Ph.D. Thesis*, Royal Institute of Technology Stockholm, **2005**.
- [22] A. T. Paradzah, E. Omotoso, M. J. Legodi, F. D. Auret, W. E. Meyer, M. Diale, *J. Electron. Mater.* **2016**, 45, 4177.
- [23] A. A. Lebedev, K. S. Davydovskaya, A. N. Yakimenko, A. M. Strel'chuk, V. V. Kozlovskii, *Tech. Phys. Lett.* **2017**, 43, 1027.
- [24] G. P. Summers, E. A. Burke, P. Shapiro, S. R. Messenger, R. J. Walters, *IEEE Trans. Nucl. Sci.* **1993**, 40, 1372.
- [25] J. Vanhellemont, E. Simoen, C. Claeys, A. Kaniava, E. Gaubas, G. Bosman, B. Johlander, L. Adams, P. Clauws, *IEEE Trans. Nucl. Sci.* **1994**, 41, 1924.
- [26] P. Hazdra, S. Popelka, *Mater. Sci. Forum* **2017**, 897, 463.